A Proposed Conceptual Model of the Process Variables Related to Heat Generation in Friction Stir Welding of Aluminum

Kevin J. Colligan

Concurrent Technologies Corporation
27980 Kim Drive, Harvest, Alabama 35749, USA

Abstract

Detailed study of the friction stir welding (FSW) process has led to a better understanding of how the process works in terms of material flow and heat generation mechanisms. However, no publications have comprehensively described the relationships between the different processing variables and how these variables affect key process conditions, such as temperature distribution, material conditions at the welding tool, etc. This paper seeks to describe the relationships between the independent process variables, such as travel speed, spindle speed and anvil condition, and the dependent process results, such as the spindle torque, heat generation and workpiece temperature distribution. The conceptual model proposed here, revised from an earlier version to distinguish between heat generated by friction and heat generated by plastic work, relates the main processing variables by showing the influence of physical effects on heat generation in the workpiece. Case studies are used to confirm and explore the relationships expressed in the conceptual model.

Introduction

It is important for users of FSW to have a conceptual understanding of how the process works. Such an understanding is helpful in deciding how to change process conditions to achieve desired effects, such as for improving joint strength, for eliminating certain common weld defects, and for transferring a known welding procedure to new conditions. Computer based models and empirical studies of the stir welding process have been developed by many researchers to examine heat transfer, metallurgical evolution, and material flow. This work has been very useful for building an understanding of the different physical effects in FSW. A general examination of the relationships between variables can now be used to develop a conceptual model of the process. In spite of the apparent simplicity of the process, interaction between process variables, which sometimes compete to produce counterintuitive results, complicates developing a conceptual understanding of the effects of the process variables. The goal of this paper is to propose a conceptual model that relates the different process variables with key process conditions in a way that will allow the practitioner of FSW to develop a general understanding of the process.

Conceptual Model Formulation

A conceptual model is proposed that relates the main process variables, structured around the interrelation of the main categories of physical effects that come into play in the generation and distribution of heat in FSW. A preliminary version of this model was published earlier [1], but the original formulation was modified to specifically distinguish the effects of friction and plastic work on the generation of heat, which is an important distinction [2]. The physical effects included in the model are metallurgical effects, mechanical effects, and heat transfer effects. As shown in Figure 1, mechanical effects are further subdivided to distinguish between effects related to the generation of torque and effects related to the generation of heat. At this level the model is very simple and it offers an intuitive way of relating the physical effects: workpiece material properties affect the generation of torque, torque affects the generation of heat, which in turn drives heat transfer, which affects material properties in advance of the welding tool. The inherent stability of the process is reflected in the closed-loop nature of the relationships between these effects. It should be noted that the present model focuses on heat generation, and does not address the effect of process variables on the lateral and axial forces generated by the welding tool, nor does the present model address the effect of process variables on defect formation.

The four categories of physical effects can be expanded to show each of the process variables and how they interact to influence the workpiece flow stress, torque, heat generation and temperature, as shown in Figure 2. In this diagram the process variables are represented in boxes with solid borders, while the physical effects are represented in boxes with dashed borders. The arrows start at a process variable, pass through a physical effect, then terminate with a process variable.

First, the flow stress of the workpiece at the welding tool pin is the result of the thermal history, the amount of strain and the strain rate. Thermal history effects can further be subdivided into slow processes that depend on the temperature distribution in advance of the welding tool, which result in metallurgical alteration of the workpiece, and rapid heating from deformation by the pin. The relatively slow metallurgical alteration of the workpiece can be thought of as pre-conditioning that the workpiece experiences as it heats from room temperature to the temperature just in front of the pin. This pre-conditioning has the effect of reducing the effect of thermo-mechanical treatments in the base metal [3], possibly to the extent that alloys of identical composition behave essentially the same in welding. Softening from deformation heating occurs from the temperature rise that results from a combination of plastic work and friction at the surface of the welding tool pin.

Friction between surfaces has been extensively studied in the past and it has been shown that friction is strongly dependent on local conditions. For sliding friction between clean metallic surfaces at high temperatures, the friction coefficient has been shown to generally decrease with increasing temperature [4]. No detailed study of the variation of friction coefficient at the temperatures and relative velocities commonly experienced in FSW has been carried out, but for the purpose of a conceptual model, only the general trend is required. It should also be noted that the effect of the friction coefficient, μ, has been embedded in the box for friction force simply as a means of conserving space in the model layout. Strictly speaking, the friction coefficient should be a separate box just above friction force, and should be related to friction force through the equation $F = \mu N$.

The flow stress is also generally influenced by strain and strain rate. For aluminum alloys, strain hardening is a weak effect at the temperatures that are reached near the welding tool, and may therefore be ignored when considering the interaction of variables. Strain rate effects however may not be insignificant and should be considered. The influence of strain rate on flow stress is difficult to analyze since detailed knowledge of the plastic deformation process is required in order to know the strain rate at a given location. However, for the purpose of constructing this conceptual model, detailed knowledge of the plastic deformation is not required, only what physical effects and variables influence the process, so it is sufficient to assert that the strain rate is a function of the peripheral velocity of the pin and the apparent vertical velocity of the threads.

Continuing in Figure 2, flow stress and friction force lead to the development of spindle torque as the workpiece material resists tool rotation. The torque can also be related to the forward travel per feature per revolution (how much material the reentrant features on the tool surface are capturing on each revolution, equivalent to chip-load in machining) [5], and the length of the pin. The travel per feature per revolution is further dependent on the spindle speed, the travel speed, and the number of reentrant features. If the welding tool being used doesn't have reentrant features, the travel per feature per revolution can be omitted from consideration, or the number of features may be set to unity to represent deliberate or unintended orbit of the pin.

When torque is applied through rotation at a given speed, heat is generated in the workpiece. The torque can be used to calculate the power (energy per unit time) delivered to the workpiece simply by multiplying the torque by the spindle speed. The relationship between the two-dimensional temperature distribution some distance from the heat source and the power and velocity of a moving heat source was formulated by Rosenthal [6] as,

$$t - t_0 = \frac{Q_p}{2\pi k} e^{-\lambda v x} \frac{K_0(\lambda v r)}{g}, \qquad (1)$$

where,
t = temperature in the plate,

t_0 = initial temperature in the plate,

Q_p = weld power,

k = thermal conductivity of the plate,

l = 1/(2 * thermal diffusivity),

v = welding speed,

x = distance from the weld center in the direction of welding = $x - vs$,

s = time,

x = position along the joint,

r = distance from the weld center to point (x ,y)

K_0 = modified Bessel function of the second kind, 0th order, and

g = plate thickness.

This function gives a means for calculating the temperature as a function of position in an infinite plate with a moving heat source. However, for the purpose of the conceptual model the Rosenthal equation is more than is required, since a precise solution is not needed. Instead, a functional relationship between the temperature distribution, welding speed and power is needed so that one can predict the general effect of the welding speed and power on the temperature distribution. The following functional relationship is proposed:

$$t - t_0 \propto \frac{Q_p}{v} \qquad (2)$$

Note that the exponential term and the Bessel function term in (1) are both a function of welding speed. If the product of these two dimensionless terms is plotted as a function of the welding speed, as shown in Figure 3, it can be seen that the curve has a trend that is similar to 1/v. Although these two functions are certainly not equal to each other, they both trend similarly downward with increasing welding speed. For the purpose of a conceptual model, the specific energy, or energy input per unit length of weld, $\frac{Q_p}{v}$, sufficiently describes the variation in the temperature distribution with welding speed and weld power, but is much simpler than the Rosenthal solution, or other similar analytic solutions, and is therefore a more convenient indicator of the temperature distribution. The specific energy can be calculated and displayed in real time on any welding machine that has a means of measuring spindle torque, spindle speed, and travel speed. The effects of plate thickness and workpiece thermal conductivity, included in equation (1) will be accounted for elsewhere in the conceptual model.

The variation in maximum workpiece temperature near the welding tool with respect to welding speed is not well represented by the specific energy in experimental results. Instead, the weld power is proposed as an indicator of maximum temperature, which is demonstrated in the case studies to follow. The welding speed certainly has an effect on the maximum temperature, but this effect influences the maximum temperature indirectly through change in the flow stress, friction, and torque that accompanies the change in welding speed.

Returning to discussion of Figure 2, the temperature distribution is the result of the balance between heat generation and heat loss to the environment. Important variables in the determination of the temperature distribution are the thermal diffusivity of the workpiece and anvil, the size of the workpiece and anvil and the workpiece surface convection characteristics. The effect of thermal conductivity (directly proportional to the diffusivity) and plate thickness from the Rosenthal temperature solution, equation (1), above, is included here in the conceptual model. The maximum temperature is not linked to the flow stress in Figure 2, since this effect is already captured in the deformation heating effect, discussed above.

A comment should be made here regarding the dual nature of heat generation in FSW. Heat is generated in FSW both by friction and by plastic work, depending on if there is local relative motion between the tool and the workpiece, generating frictional drag at the interface, or if there is local seizure. Local seizure can be the result of certain reentrant features cut into the surface of the tool, such as flats or grooves, or can be from certain

complex tool motions that are not based on pure rotation [7, 8, 9]. These two heat generation mechanisms may coexist at any given time in different regions of the tool. While it is difficult to experimentally isolate the proportion of heat generation attributable to each of these mechanisms, both mechanisms have been experimentally observed [10] and numerical model results have attributed heat generation to both mechanisms being simultaneously present [11].

Conceptual modeling of the relationships between the variables can be further enhanced by showing whether the relationship is a direct relationship or an inverse relationship, as shown in Figure 4. In this diagram the relationship is coded as a plus sign for a direct relationship and a minus sign for an inverse relationship. As will be seen in the case studies that follow, the relationships between variables can be used to help understand how changing welding conditions will influence the key features of flow stress, torque, heat generation and workpiece temperature. These case studies were gathered from existing weld data and analyzed in terms of the variable relationships model shown in Figure 4, both for the purpose of explaining what was observed in the testing and for confirming the formulation of the model.

Two published papers were used in the case studies that follow [5, 12]. These were supplemented by data from unpublished work performed by the author and by the work by Reynolds and Tang [3]. Aluminum alloy 5083, a non-heat treatable, solution strengthened alloy, was used in the published studies and aluminum-lithium alloy 2195 was used in the unpublished work. The nominal alloy compositions are shown in Table 1. In the first published study, 25.4-mm 5083-H131 aluminum plate was welded using different spindle speeds, travel speeds, and using pins with different numbers of features (in this case, the reentrant features were flats cut into the surface of a threaded pin) in order to isolate the effects of travel per feature per revolution, spindle speed and travel speed. The welds performed are listed in Table 2, and the tool design used is summarized in Table 3. In the second published study, welds were made in 25.4-mm 5083-H116 with embedded thermocouples to measure the mid-plane temperature of the workpiece as the welding tool approached and passed. Welds were made at different travel speeds, with different shoulder diameters and with different anvil conditions (mica insulated vs. non-insulated). A summary of the welding conditions is presented in Table 4. The tool design was identical to the tool used in the Colligan study, summarized in Table 3, except that a pin with four flats was used in all of the welds made.

Case Study 1 – Changing Travel Speed

Three main sets of findings are used here to examine the effect of changing travel speed on heat generation in FSW of aluminum. In the first study, by Colligan [5], welds were made with increasing travel speed while maintaining constant spindle speed and travel per feature per revolution. The spindle torque was measured and used to calculate the weld power and weld specific energy (heat input per unit length of weld), as shown in Figure 5. As can be seen in the figure, when the travel speed was increased the torque and weld power were seen to increase and the weld specific energy was observed to decrease. From the study by Xu [12] in welds that had a mica-insulated anvil, Figure 6 shows that increasing travel speed has the effect of decreasing the temperature away from the welding tool and increasing the maximum temperature recorded on the thermocouple. The torque, specific energy, and weld power measured in the Xu study are plotted in Figure 7. The trend of this data is similar to that observed in the Colligan study. The slight differences between the two studies are presumably due to the fact that in the Xu study an insulated anvil was used, and no attempt was made to hold the travel per flat per revolution constant as the travel speed increased. Finally, in an unpublished experiment a weld in 0.725-inch thick 2195 plate was started at 127 mm/min travel speed and then the travel speed was increased to 152 mm/min. It was observed that the torque and weld power increased, but it took a full 75-mm of travel before the full effect was observed, as shown in Figure 8.

The observations from these studies can be explained by looking at the influence of increasing travel speed on the key physical effects, as shown in Figure 9. In this figure, upward influence on a variable is represented by a heavy black line, downward influence on a variable is represented by a heavy gray line, a neutral influence is represented by a heavy

dotted line, and an unaffected influence is left as a thin black line. The five points below correlate with the numbers in the figure.

1. First, it is known from experiment that torque goes up with increasing travel speed, as pointed out in Figure 5 and in Figure 7. This increases the weld power, since the spindle speed is unchanged, and simultaneously exerts an upward influence on the specific energy. However, the increase in travel speed also exerts a downward influence on the specific energy. In the Colligan and Xu studies, the competition between these variables was dominated by the travel speed, since the specific energy was seen to decrease with increasing travel speed. This effect was also observed by Reynolds and Tang [3]. This must always be the case, since if the specific energy increased with increasing travel speed (in response to increasing torque), the ultimate result would be decreasing torque, which would make increasing specific energy impossible.
2. The increase in weld power is reflected in the increased maximum temperature observed in the Xu study, shown in Figure 6.
3. The decreased specific energy resulted in a lower temperature distribution away from the weld zone, also observed by Xu, since the workpiece and anvil heat loss characteristics were not changed.
4. The reduced temperature distribution has the effect of increasing the flow stress of material arriving at the pin, since there is presumably less metallurgical alteration from precipitate coarsening and dissolution and possibly less softening from recovery.
5. The increased travel speed also has the effect of increasing the force on the welding tool in the direction of welding and the plunge force (along the tool's rotational axis), as was observed in the study by Reynolds and Tang [3]. This has the effect of exerting an upward influence on the frictional force in areas of the tool where sliding occurs between the tool and the surrounding workpiece material. It is conceivable that the reduced temperature distribution and increased flow stress in the workpiece material as it initially contacts the pin would have the effect of increasing the friction coefficient as well, further increasing the net friction force exerted tangentially at the sliding interfaces.
6. The increased flow stress and frictional force results in increased torque, in agreement with 1, above.

In the Colligan study, the influence of changing travel speed on the travel per flat per revolution was neutralized by changing the number of pin flats. In the Xu study this was not done, so increasing the travel speed should have increased the travel per flat per revolution, exerting an additional upward influence on the torque. So in the Xu study the effects of flow stress and travel per flat per revolution combine to increase the torque.

Force data collected in the Colligan study is not a good example of the effect of travel speed, since in that study the number of flats cut into the pin surface was changed to give constant travel per flat per revolution, thus changing the surface area of the pin that had threads. In the study by Reynolds and Tang, referenced in point 5 above, travel speed changes were made without changing the number of pin features, giving a better example of the effect of travel speed on welding forces.

In the case of the weld in 0.725-in 2195-T8, it was observed that it took about 75-mm of travel for an increase in travel speed to have the full effect on changing the torque. This result is in agreement with Figure 9, since the increase in torque is the result of the reduced temperature away from the weld zone, which results in reduced metallurgical alteration, which takes time to develop as the tool travels.

Case Study 2– Changing Spindle Speed

The conceptual model was recently published using a case study that specifically examined the effect of changing spindle speed [2]. Additional examination of this effect is made here. In the Colligan study [5], welds were performed to evaluate the effect of increasing spindle speed on the torque, specific energy, and weld power while keeping the travel per feature per revolution and the travel speed constant, as shown in Figure 10. It was observed that increasing the spindle speed dramatically reduced the spindle torque. The weld power and specific energy increased significantly at first, but reached a limiting value. In an unpublished experiment by the author, a weld in 25.4-mm 2195-T8P4 was

started at 170 rev/min, then the spindle speed was increased to 200 rev/min while keeping the travel speed constant, as shown in Figure 11. The spindle torque was seen to immediately drop in response to the increased spindle speed, and it took just two data samples (about 2 seconds) for the torque change to reach its full effect. These observations can be examined within the context of the conceptual model, shown in Figure 12.

1. It was observed in Figure 10 that increasing the spindle speed resulted in decreased torque, which, according to the conceptual model, would exert a downward influence on the power and specific energy.
2. The increase in spindle speed also exerts an upward influence on the power and specific energy, and it was observed that initially these variables increased, but then reached a limiting value of about 10 kW for the power and about 5 kJ/mm for the specific energy. The increasing power and specific energy would be expected to have the effect of increasing the maximum temperature and the overall temperature distribution as long as the power and specific energy are increasing, but no such test data was available to confirm this prediction in the model. However, in a study by Record, et al. [15], it was concluded that spindle speed was the most significant factor in determining welding tool temperature, supporting the prediction that increasing spindle speed leads to increased power and specific energy and increasing workpiece temperature.
3. Since no change was made to the heat loss characteristics, one would expect the increasing spindle speed to increase the temperature distribution, but only to a limited value, since the specific energy reaches a limited value. Presumably this limitation is related to the melting point of the workpiece material, where the flow stress reaches zero. The increasing spindle speed would therefore be expected to increase metallurgical alteration and thereby decrease the flow stress to a point, but above 333 rev/min in this specific case (weld PE6 in Table 2 and Figure 10), there should be no additional increase in temperature or in metallurgical softening.
4. Increasing the spindle speed has the effect of increasing thermal softening from deformation heating, exerting an additional downward influence on the flow stress and friction coefficient at the tool. This effect is counteracted, to some unknown extent, by the presumed increase in strain rate and local compressive force. However, if it is known that the torque goes down with increasing spindle speed (Figure 10), even beyond the point at which no additional far-field temperature distribution increase is expected, it must be the case that the deformation heating effect is stronger than the effects of increasing strain rate and local compressive force, resulting in a continued decreased flow stress with increasing spindle speed. Since the torque was observed to steadily decrease with increasing spindle speed in this and other studies [2], it is conceivable that the decrease in torque is primarily due to deformation heating, with increased metallurgical alteration and strain rate effects being secondary.
5. A recently published study [2] showed that with increasing spindle speed the in-plane compressive force against the tool increases for spindle speeds above some value. This would tend to have a positive effect on the friction generated, but ultimately we know from the data collected that the torque decreased with increasing spindle speed, so it must be that the increase in local compressive force has, at best, a regulatory effect on the total torque generated in this case.
6. Since the effect of travel per flat per revolution was neutralized in the Colligan study by changing the number of flats on the pin, the decreased flow stress results in decreased torque, which is in agreement with 1, above.

There is further evidence that the decrease in flow stress must not be entirely due to an elevated temperature distribution (and the resultant metallurgical alteration) with increasing spindle speed. In the unpublished experiment in 25.4-mm 2195 aluminum-lithium, it was observed that increasing the spindle speed resulted in an immediate change in the spindle torque. This would not be the case if the decrease in flow stress were the result of metallurgical alteration, which takes time to develop.

The strain rate sensitivity, which one would expect to increase flow stress with increasing spindle speed, apparently does not significantly affect FSW of aluminum, presumably because the plastic deformation is not isothermal. In the absence of rate

sensitivity, increasing spindle speed reduces the flow stress through deformation heating and thermal softening, resulting in a decrease in torque.

Case Study 3 – Changing Anvil Insulation Condition

In the Xu study, tests were also carried out to examine the effect of different anvil conditions on the temperature field in friction stir welds. A solid anvil and an anvil insulated by mica were both used with identical weld settings. Thermocouples were used at mid-plane in the plate of 25.4-mm 5083-H131 aluminum to record the temperature distribution in the plate during welding. The mid-plane temperature as a function of position for the two welds is shown in Figure 13. The data showed that insulating the anvil had the effect of raising the far-field temperature distribution but lowering the mean maximum temperature. The torque, specific energy and weld power for these two welds are tabulated in Table 4. This result is instructive since it shows the effect of changing the far-field temperature distribution without changing the independent process variables. The observed effects can be examined within the context of the conceptual model, shown in Figure 14.

1. Adding anvil insulation had the effect of reducing the thermal diffusivity, which reduced the heat lost and, through the inverse relationship to temperature distribution, it increased the temperature distribution in advance of the tool.
2. Increased temperature distribution had the effect of increasing metallurgical alteration, reducing the flow stress of the workpiece as it arrives at the pin. No other process variables were changed, so the change in temperature distribution has a direct effect on flow stress.
3. The reduced flow stress resulted in decreased torque, as shown in Table 4.
4. The reduced torque resulted in decreased weld power and specific energy, also shown in Table 4.
5. The reduced weld power would be expected to result in decreased maximum temperature, which is seen in Figure 13. The reduced specific energy did not result in reducing the temperature distribution, apparently since this effect was overpowered by the change in anvil condition noted in 1.

The increased temperature distribution in advance of the tool has the effect of increasing the softening the workpiece material by metallurgical alteration effects, which decreased the flow stress, the torque, the weld power, and the peak temperature. It is speculated that this same situation could be achieved by reducing the workpiece size (such as by welding very narrow plates), by reducing the anvil size, or by making bobbin or self-reacted welds (where the anvil is eliminated). This also highlights the critical nature of workpiece and anvil size effects, which becomes an important consideration when optimizing an application in the laboratory environment on a reduced-size workpiece for subsequent transition to production of larger components.

It was noted in observation 5 above that the competition between reduced specific energy (tending to lower the temperature distribution) and reduced heat loss (tending to increase the temperature distribution) was dominated by the reduced heat loss. In the work by Reynolds and Tang [3], a similar competition existed when it was noted that aluminum alloy 6061 had the highest specific energy of all the alloys tested in identical conditions. It was speculated that this was due to 6061 having the highest thermal conductivity of the alloys tested. In the conceptual model proposed here, increased workpiece thermal conductivity leads to increased heat loss, decreased temperature distribution, increased flow stress and friction coefficient, increased torque, and increased specific energy, which is in competition with the increased thermal conductivity for the determination of the temperature distribution. Apparently, the increasing specific energy acts to mitigate the decrease in temperature distribution produced by increasing workpiece thermal conductivity, much in the way that the negative effect of increasing spindle speed on the friction and flow stress was mitigated by increasing compressive force against the tool. Intuitively, in the case of increasing thermal conductivity it is impossible for the increased specific energy to result in increased temperature distribution, overpowering the effect of increased heat loss, since this would result in decreased flow stress and friction, decreased torque, and decreased specific energy.

Conclusions

A conceptual model is proposed to relate the process variables and physical effects in FSW of aluminum and its alloys. This model provides a framework for examination of the effect of changing process conditions, so that a better intuitive understanding of the FSW process can be developed. Three case studies were examined within the context of the conceptual model to test the model against experimental observations. The case studies were found to generally be consistent with the proposed model, and in some situations the case studies showed how competition between variables resulted in different outcomes. Perhaps as more case studies are examined, experience will dictate how to assign weights to different effects as an aid to predicting the result of competition between different variables.

References

1. Colligan, K.J., "Relationships Between Process Variables related to Heat Generation in Friction Stir Welding of Aluminum," *Friction Stir Welding and Processing IV*, ed. Mishra, R., TMS, 2007, pp. 39-54.
2. Colligan, K.J. and Mishra, R.S., "A Conceptual Model for the Process Variables Related to Heat Generation in Friction Stir Welding of Aluminum," *Scripta Materialia*, 58(2008), 327-331.
3. Reynolds, A.P., and Tang, W., "Alloy, Tool Geometry, and Process Parameter Effects on Friction Stir Weld Energies and Resultant FSW Joint Properties," *Friction Stir Welding and Processing*, ed. Jata, K.V., Mahoney, M.W., Mishra, R.S., Semiatin, S.L., and Field, D.P., TMS, 2001, pp. 15-23.
4. Bowden, F.P. and Hughes, T.P., *Proceedings of the Royal Society of London*, A, 172 (1939), 263.
5. Colligan, K.J., Xu, J., and Pickens, J.R., "Welding Tool and Process Parameter Effects in Friction Stir Welding of Aluminum Alloys," *Friction Stir Welding and Processing II*, ed. Jata, K.V., Mahoney, M.W., Mishra, R.S., Semiatin, S.L., and Lienert, T., TMS, 2003.
6. Rosenthal, D., "Mathematical Theory of Heat Distribution During Welding and Cutting," *Welding Journal*, 1941, 20(5), 220s-243s.
7. Thomas, W.M., Staines, D.G., Norris, I.M., and de Frias, R., "Friction Stir Welding – Tools and Developments," presented at FSW Seminar, Instituto de Soldadura e Qualidade, Porto, Portugal, Dec. 3, 2002.
8. Dawes, C.J. and Thomas, W.M., Proceedings of the 1st International Symposium on Friction Stir Welding, Thousand Oaks, Ca., June 14-16, 1999.
9. Colegrove, P.A. and Threadgill, P.L., "Development of the Trivex Friction Stir Welding Tool," The Welding Institute, published on the Internet, Feb. 20, 2003.
10. Colligan, K.J. and Chopra, S.K., Proceedings of the 5th International Symposium on Friction Stir Welding, Metz, France, September 14-16, 2004.
11. Colegrove, P.A., Shercliff, H.R., and Threadgill, P.L., Proceedings of the 4th International Symposium on Friction Stir Welding, Park City, Utah, May 14-16, 2003.
12. Xu, J., Vaze, S.P., Ritter, R.J., Colligan, K.J., and Pickens, J.R., "Experimental and Numerical Study of Thermal Process in Friction Stir Welding," International Conference on Joining of Advanced and Specialty Materials VI, ASM, 2003.
13. Department of Defense, Military Standard, "Detail Specification: Armor Plate, Aluminum Alloy, Weldable 5083 and 5456," MIL-DTL-46027J, September 4, 1998.
14. Brown, W. F., Jr., Aerospace Materials Handbook, Nonferrous Alloys – AlWT 2195, p.6.
15. Record, J.H., Covington, J.L., Nelson, T.W., Sorensen, C.D., and Webb, B.W., "Fundamental Characterization of Friction Stir Welding," Proceedings of the 5th International Symposium on Friction Stir Welding, September, 2004, Metz, France.

Table 1. Specified chemical composition ranges for aluminum alloys 5083 and 2195.

Alloy	Chemical Compositions, wt. %												Impurities, %	
	Cu	Mn	Mg	Fe	Si	Zn	Ti	Cr	Zr	V	Ag	Al	Each	Tot.
5083 [13]	0-0.10	0.40-1.00	4.0-4.9	0-0.40	0-0.40	0-0.25	0-0.15	0.05-0.25	-	-	-	Bal.	0.05	0.15
2195 [14]	3.70-4.30	0-0.25	0.25-0.80	0-0.15	0-0.12	0-0.25	0-0.10	-	0.08-0.16	-	0.25-0.60	Bal.	0.05	0.15

Table 2. Summary of welding conditions, welds in 25.4-mm 5083-H131 [5].

Weld Identification	Spindle Speed rev/min	Travel Speed mm/s (in/min)	Number of Pin Features (flats)	Travel per Feature per Rev. mm/feature-rev (in/feature-rev)
PE1	250	2.12 (5.0)	4	0.127 (0.0050)
PE2	250	2.12 (5.0)	3	0.170 (0.0067)
PE3	250	2.12 (5.0)	2	0.254 (0.0100)
PE4	250	1.59 (3.7)	3	0.127 (0.0050)
PE5	250	1.06 (2.5)	2	0.127 (0.0050)
PE6	333	2.12 (5.0)	3	0.127 (0.0050)
PE7	500	2.12 (5.0)	2	0.127 (0.0050)
PE8	250	2.12 (5.0)	0	0.508[1] (0.0200)

[1]mm/rev

Table 3. Tool design for welds in 1-in 5083-H131 [5].

Shoulder Diameter, mm (in)	42 (1.65)
Scroll Depth, mm (in)	1.3 (0.05)
Scroll Pitch, mm (in)	3.3 (0.13)
Scroll Width, mm (in)	2.5 (0.10)
Nominal Pin Length, mm (in)	25.2 (0.992)
Pin Maximum Diameter, mm (in)	15.2 (0.598)
Thread Pitch, mm (in)	1.41 (0.056)
Number of Features (flats)	0, 2, 3 and 4

Table 4. Summary of welding conditions, welds in 25.4-mm 5083-H116 [12].

Plate Number	Spindle Speed rev/min	Travel Speed mm/s (in/min)	Insulating Conditions	Torque N-m (ft-lbs)	Specific Energy kJ/mm (BTU/in)	Power kW
Plate 02	250	2.12 (5.0)	With mica	326 (240)	3.6 (97)	8.5
Plate 08	250	2.12 (5.0)	no mica	369 (272)	4.1 (110)	9.7

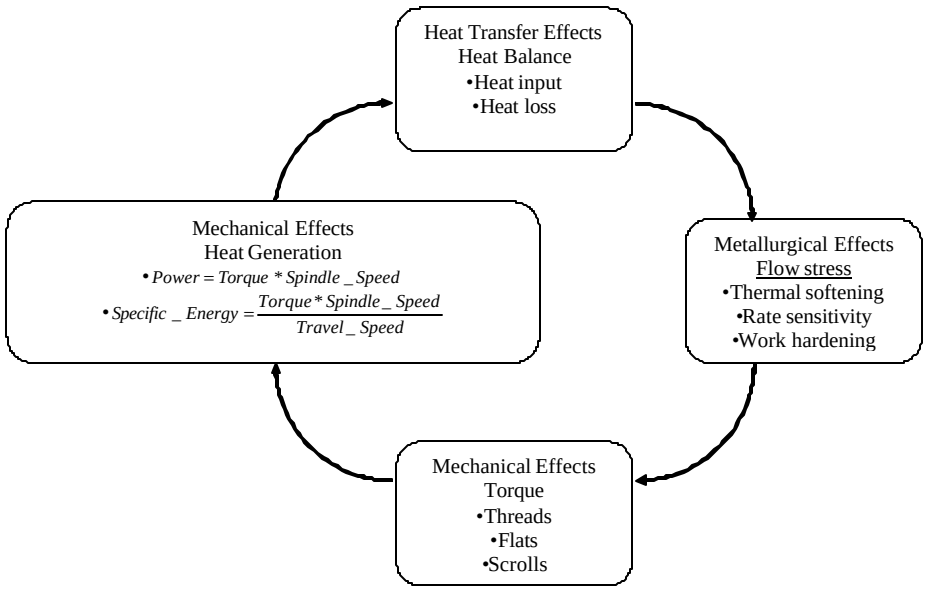

Figure 1. Relationships between the main groups of physical effects.

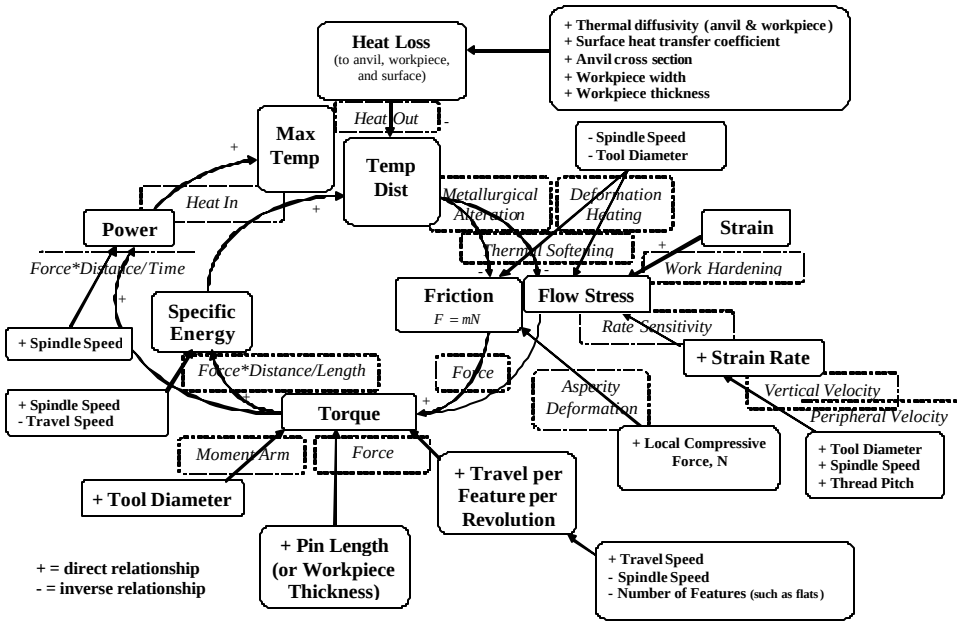

Figure 2. Relationships between variables with physical effects overlaid.

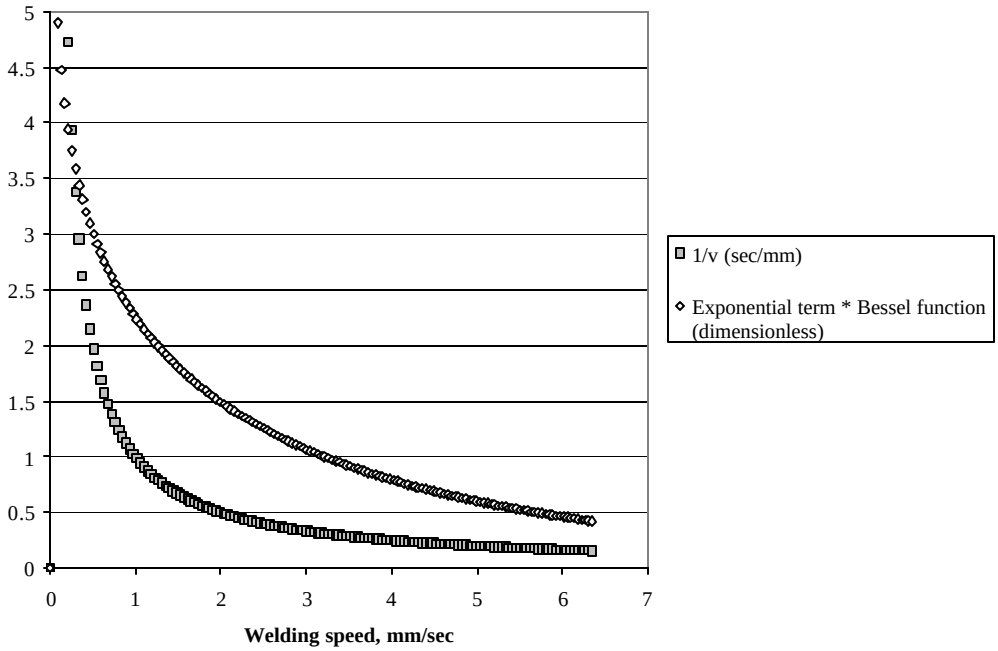

Figure 3. Comparison between 1/v and the product of the exponential term and the Bessel function from Rosenthal's two-dimensional temperature solution.

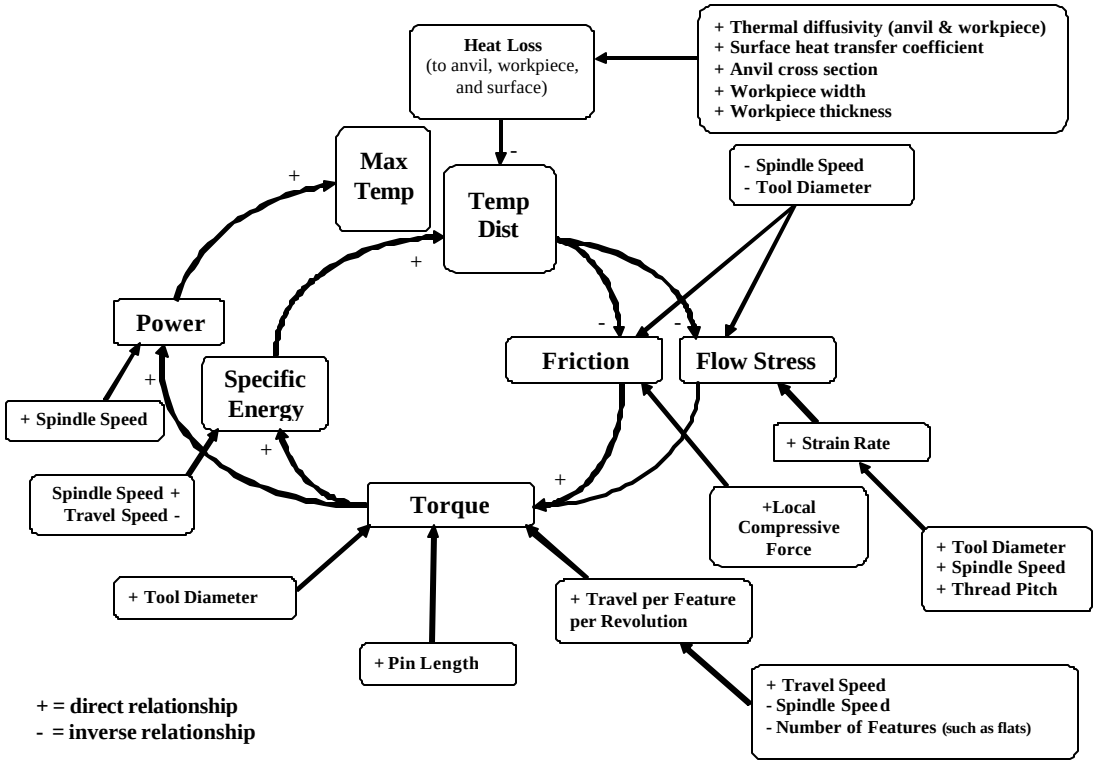

Figure 4. Relationships between variables.

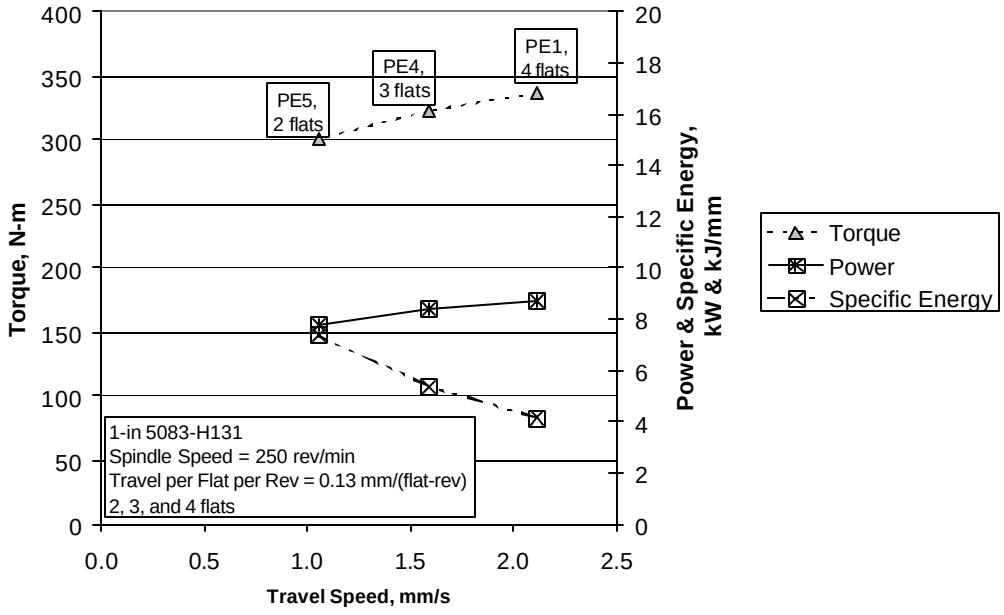

Figure 5. Torque, Power, and Specific Energy as a function of travel speed, weld in 25.4 - mm 5083-H131 aluminum plate [5].

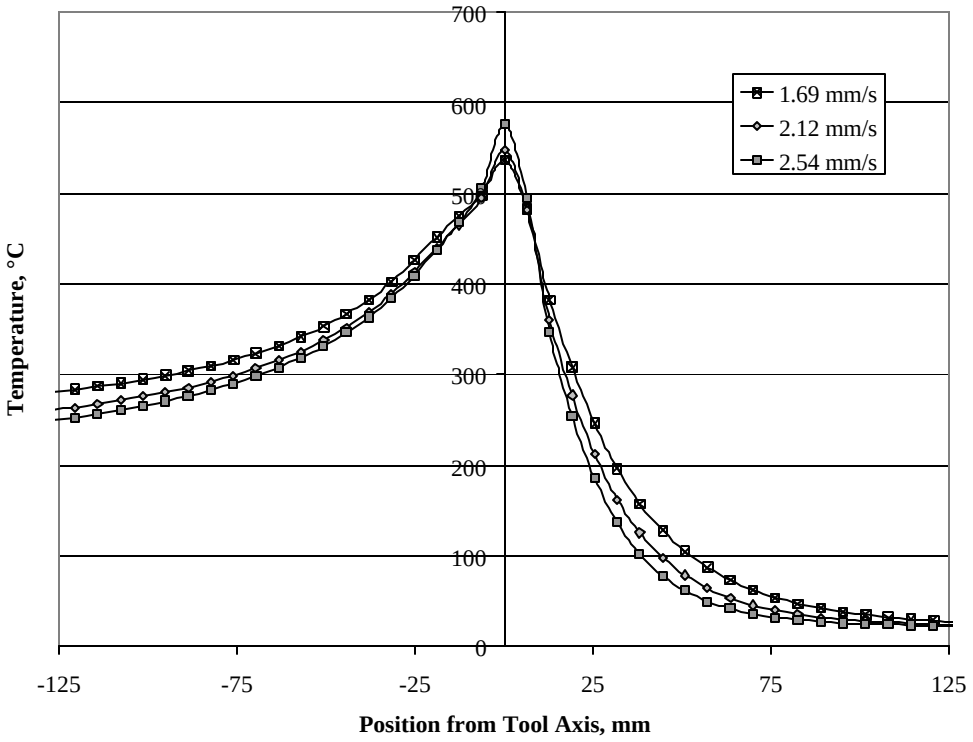

Figure 6. Temperature at plate mid-thickness as a function of position, friction stir weld in 25.4-mm 5083-H116 plate [12].

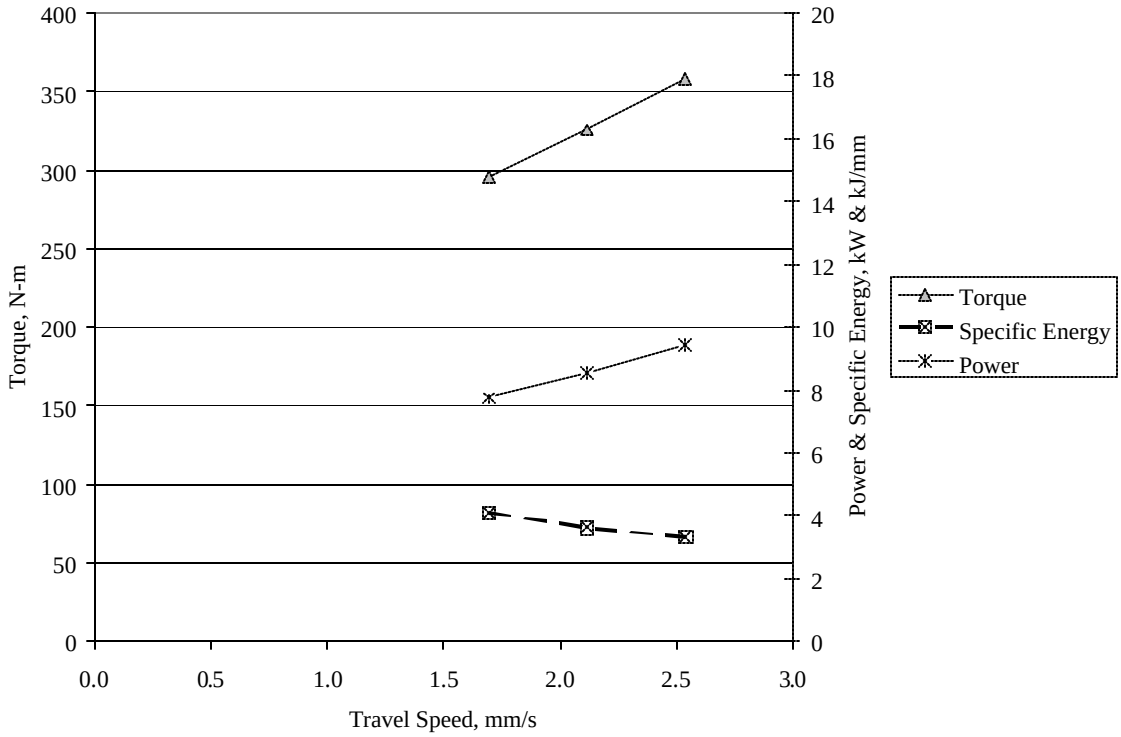

Figure 7. Torque, power, and specific energy as a function of welding speed, friction stir welds in 5083-H116 aluminum plate [12].

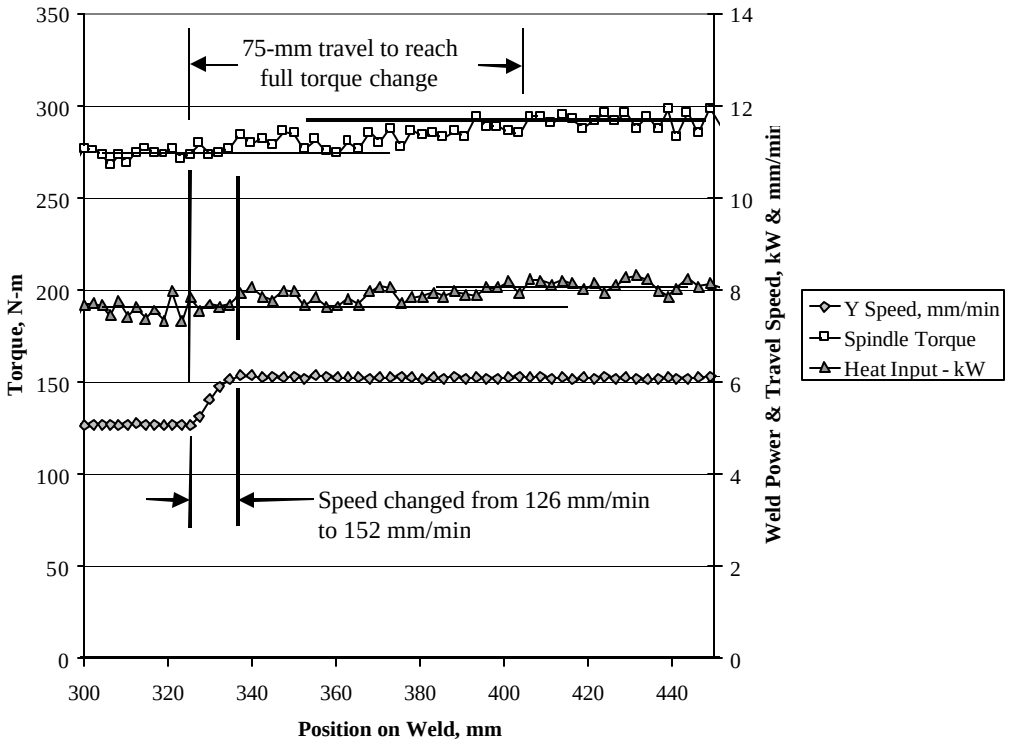

Figure 8. Torque, weld power, and travel speed as a function of position on the weld from FSW of 25.4-mm 5083-H116 aluminum plate, showing sudden increase in travel speed.

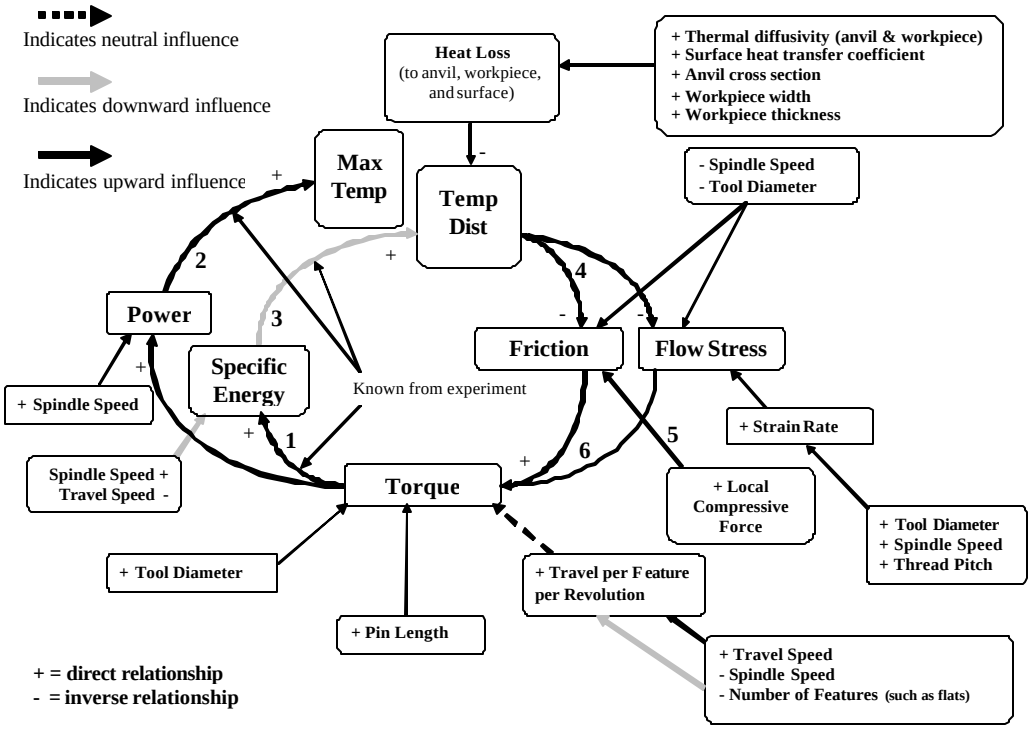

Figure 9. Influence between variables for increasing travel speed.

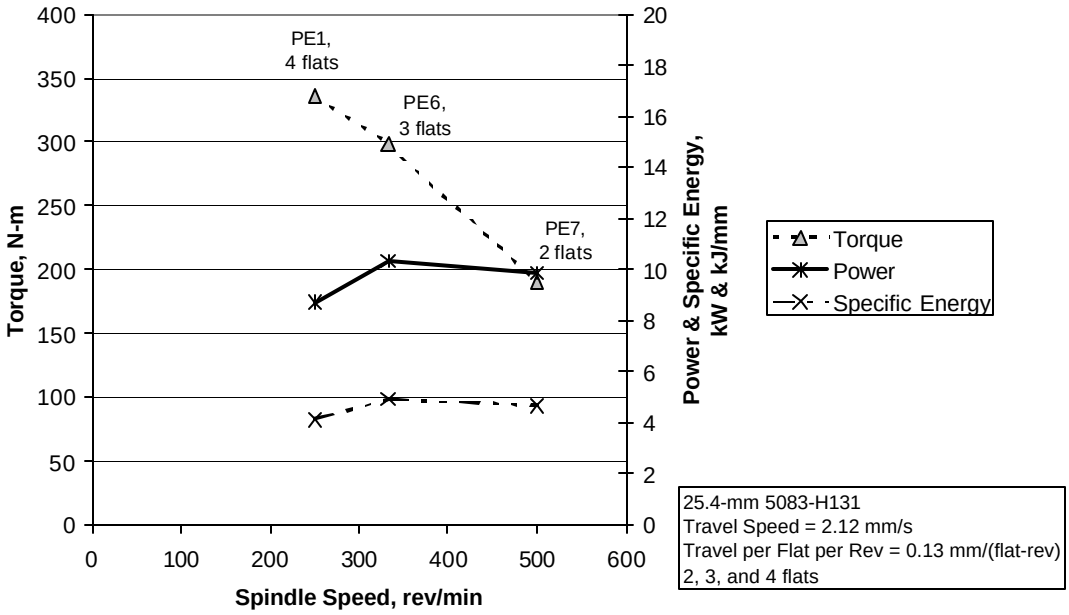

Figure 10. Torque, weld power, and specific energy as a function of spindle speed, friction stir welding of 25.4-mm 5083-H131 aluminum plate.

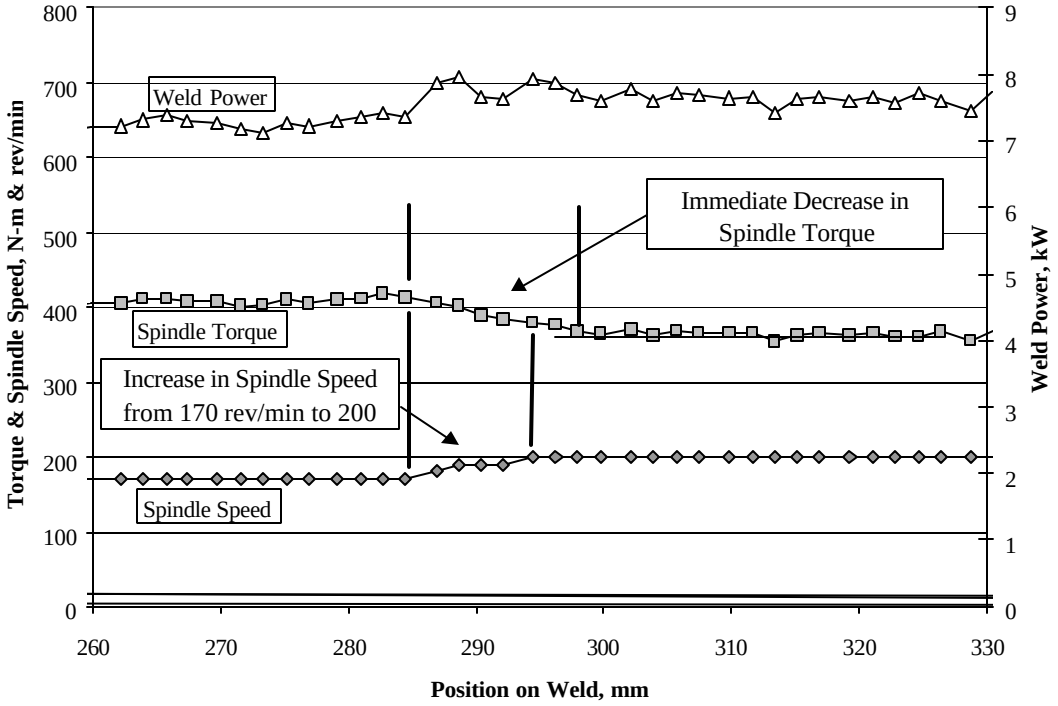

Figure 11. Torque, spindle speed, and weld power as a function of position on weld from friction stir weld in 25.4-mm 2195-T8, showing the effect of a change in spindle speed.

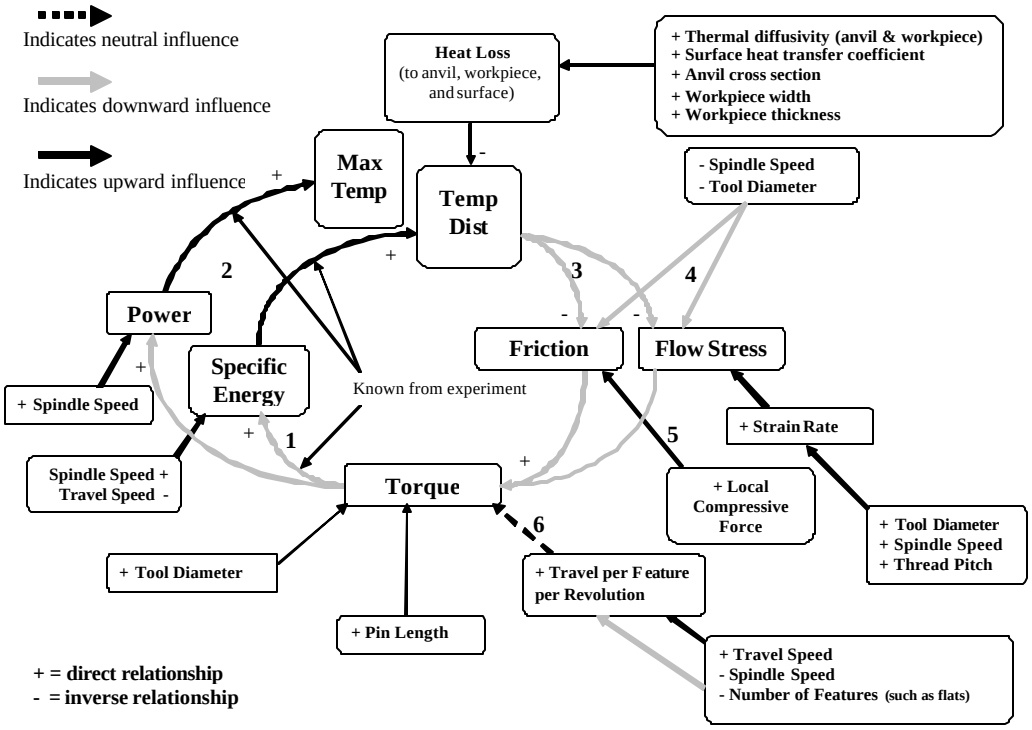

Figure 12. Influence between variables for increasing spindle speed.

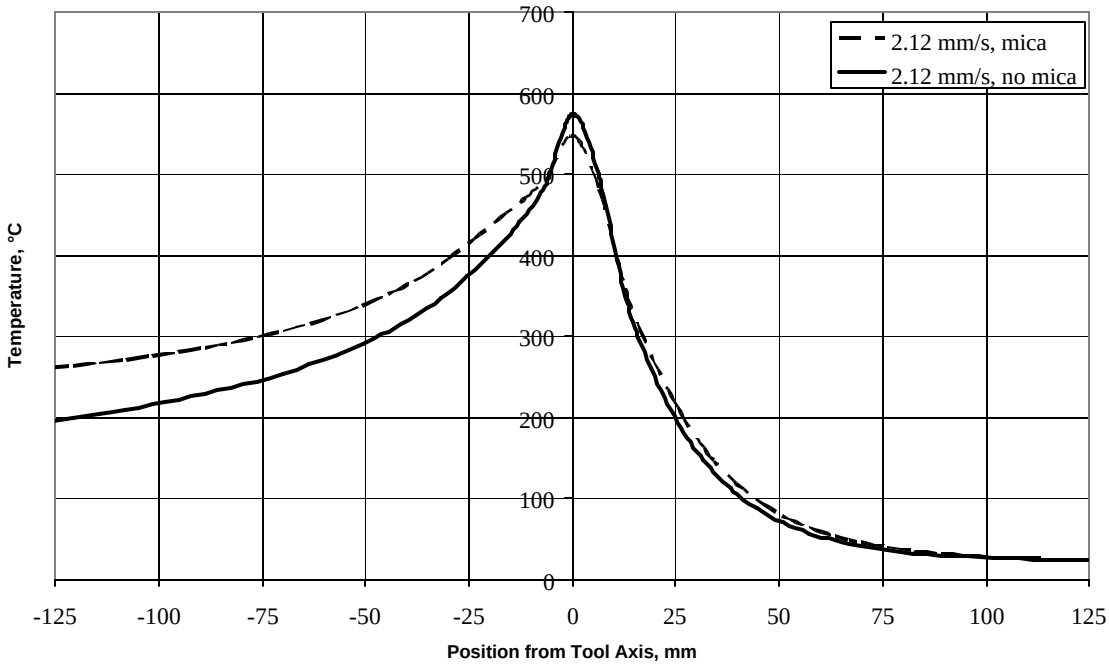

Figure 13. Plate mid-plane temperature as a function of time for friction stir welding of 25.4-mm 5083-H131 aluminum plate, showing the effect of anvil insulation.

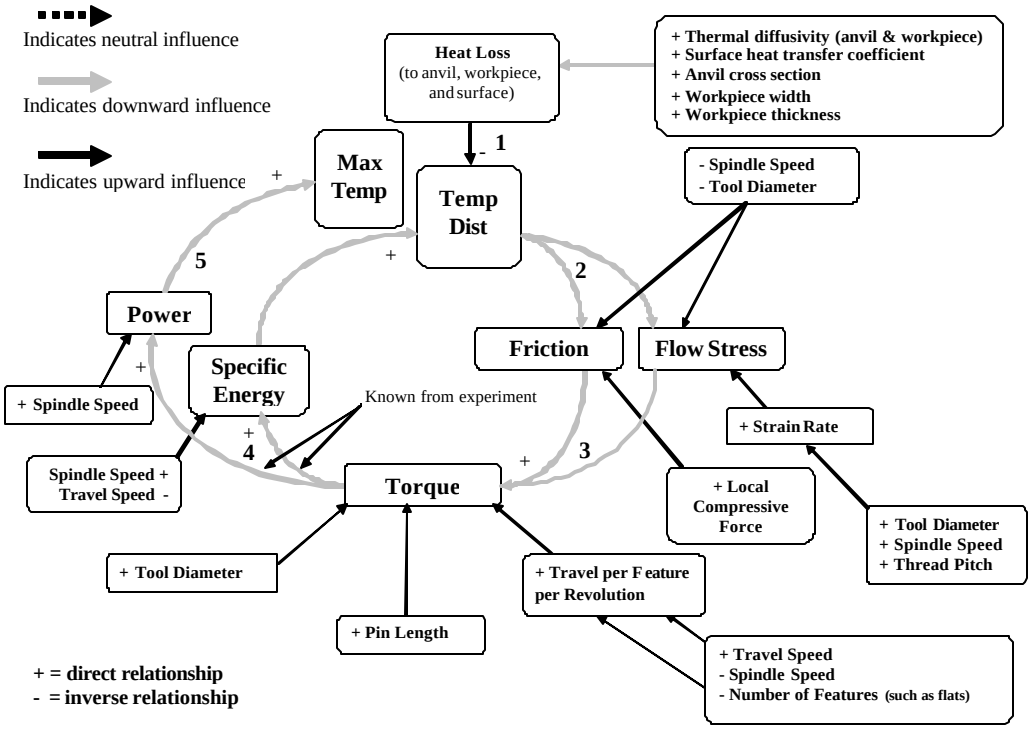

Figure 14. Influence between variables for adding anvil insulation.